ISSN 2522-4182

DOI: 10.32347/2522-4182.18.2026.184-201
УДК 624.042

COMPARISON OF OVERPRESSURE ON FLOOR SLABS UNDER BLAST LOADING AT SMALL DISTANCES FROM THEIR SURFACE

Mykyta Biliaiev

Kyiv National University of Construction and Architecture
31, Povitryanykh Syl Ave., Kyiv, Ukraine, 03037

[1]biliamyk@gmail.com, https://orcid.org/0009-0000-1027-9285

Abstract. The article is devoted to the study of excess (over)pressure acting on building floor slabs when an explosion occurs at short distances from their surface The relevance of the work is due to the fact that the current codes and calculation practices, in particular the provisions of the UFC 3-340-02 and M. Sadovskiy formulas, are mainly focused towards larger distances from the explosion and do not take into account a local nature of the load that arises in the case of a close detonation. This potentially leads to significant deviations in assessing the real level of blast impact on structural elements.

The aim of the study is to develop and approximate a realistic relationship between the peak overpressure, the distance to the floor surface, and the mass of the explosive charge for explosions at distances up to 2 m. To achieve this goal, a series of numerical experiments was performed using the Ansys software package. The computational model represents a composite steel–reinforced concrete floor slab with overall dimensions of 12 × 6 m, supported by steel beams with perforated webs, first considering all structural components and later in a simplified form with different slab thicknesses. TNT-equivalent charges of 50, 75, and 100 kg were considered at stand-off distances of 0.5, 1.0, 1.5, and 2.0 m from the surface.

Obtained results demonstrates that most commonly used codes significantly overestimate the peak pressure at short distances: by 4–9 times according to UFC 3-340-02 and by 2–5 times according to M. Sadovskiy formulas compared with the numerical simulation. A significant influence of the slab stiffness on the pressure magnitude was revealed. It was established that the pressure-distance relationship has a distinct nonlinear dependency, while the dependence on the explosive mass is almost linear.

Based on the obtained data, new analytical relationships for estimating the peak overpressure are proposed, including a generalized formula using scaled distance parameter adapted for explosions at short distances. The proposed expressions were validated against series of numerical experiments and can be used for engineering assessment of blast loads on floor slabs at close distances from their surface. In addition, the failure patterns of the structure were studied, and the main directions for strengthening were identified: increasing the slab thickness and improving the anchorage of steel beams to prevent uplift and separation.

Mykyta BILIAIEV
PhD student,
Department of Steel and Timber Structures,
MEng.

Keywords: blast loading; composite structures; hybrid structures; cellular beams; overpressure.

INTRODUCTION

Traditional approaches to assessment of blast loads, both abroad [1, 2] and in Ukraine [3], are focused on the averaged action on the structure as a whole and do not reflect the local effects typical for detonations at close distances [4, 5].

They are assuming explosions at relatively large distances (tens and hundreds of meters from the structure) and determining an overpressure acting on the entire structure rather than locally. According to DBN V.1.2-4:2019 [3] most shelters are required to be designed for the effect of an overpressure at the front of the air shock wave of at least $\Delta P_f = 100$ kPa (1 kg/cm²), and within the boundaries of areas and sanitary-protection zones of nuclear power facilities - $\Delta P_f = 200$ kPa (2 kg/cm²). Design requirements for critical infrastructure facilities are set at levels between $P_f = 100$ kPa (1 kg/cm²) and $P_f = 500$ kPa (5 kg/cm²), depending on their type.

Ukrainian scientific publications [6, 7, 8] in most cases refer to M. Sadovskiy formulas, although some of them include wider selection of methods [8]. General laws of explosion scaling and shock waves reflection by obstacles are systematized in engineering handbooks for blast resistant buildings [10]. UFC 3-340-02 [1] document by U.S. Department of Defens widely directly and indirectly mentioned in articles [8, 9] and guidelines makes it possible to calculate overpressure individually depending on the type of explosion (airburst, surface burst, etc.) and the distance to it. However, methods intended primarily toward large distances have a high probability for significant errors as the detonation point approaches closer to the structure. At small distances, the shock-wave front undergoes substantial deformation, and the contribution of reflected pressure increases sharply, which is not taken into account in simplified approaches suggested in commonly used codes of practice [11, 12, 13].

As a part “Hybrid floor with castellated beams under accidental (blast) loading” PhD research it was decided to additionally investigate overpressure levels created by blast at small distances from the floor surface and obtained values with existing common practices. As some of the previous numerical studies for protective structures also confirm a significant discrepancy between analytical formulas and the actual stress values for explosions at small distances [14].

RESEARCH PURPOSE AND GOALS

Purpose of this work is to approximate a realistic relationship of peak overpressure from the distance to surface and amount of explosives for detonation points up to 2 m above the slab surface. Previous studies [15, 16] have shown that for detonations at small distances local impulse on a structural element dominates over the area-averaged pressure, which justifies the need to develop separate relationships for blasts at small distances.

Goals:

- to develop a sufficiently accurate model of a composite floor slab with castellated beams subjected to a blast load with a detonation point at 0.5m above its surface;
- to study the ways in which composite floor failures under defined blast loading and make a conclusions on possible model/structural improvements and further research possibilities;
- to create a series of models simulating explosions of 50, 75, and 100 kg of TNT at distances up to 2 m from the slab surface;
- to approximate the relationships between peak overpressure and a detonation point distance to the slab for a constant (fixed) explosive charge;
- to approximate the relationships between peak overpressure and the explosive charge for a constant (fixed) detonation point distance to the slab;
- to derive a general relationship for the peak overpressure acting on the slab as a function of two parameters: detonation point distance to the slab and amount of explosives.

OVERPRESSURE CALCULATION PRACTICES ACCORDING TO UFC 3-340-02 AND M. SADOVSKIY FORMULAS

For a free spherical explosion of trinitrotoluene (TNT) in air above the ground

surface at sea level, UFC 3-340-02 [1] provides graphs of the main blast wave parameters, as shown in Fig. 1. To ensure that the relationships simultaneously account for both the distance from the explosion and the amount of explosives, the scaled distance parameter $Z$is introduced (1):

$$Z = \frac{R}{\sqrt[3]{W}}, \qquad (1)$$

where R – distance to detonation point, in feet;

W – amount of explosives in TNT equivalent, in pounds.

Basic values on these charts are the incident overpressure $P_{so}$and the reflected overpressure from a perpendicular surface P_r. In this case, both values are defined in pounds per square inch (psi).

As an example by using above method for spherical air burst of 50 kg of TNT at a distance of 0.5 m from a 12x6 m slab following overpressure values are obtained:

Detonation point distance:

$$R = 0.5m\ (1.64\ ft)$$

Amount of explosives:

$$W\ =\ 50kg\ (110.23\ lbs)$$

Scaled perpendicular distance:

$$Z = \frac{R}{\sqrt[3]{W}} = \frac{1.64}{\sqrt[3]{110.23}} = 0.342\ \frac{ft}{lbs^{1/3}}$$

$$P_r \approx 40000\ psi = 275.79MPa = \\ = 275790kPa$$

Similar values were calculated for detonation points at 1.0, 1.5, and 2.0 m from the slab surface. Results are presented in Fig. 9 and in the summary Table 1.

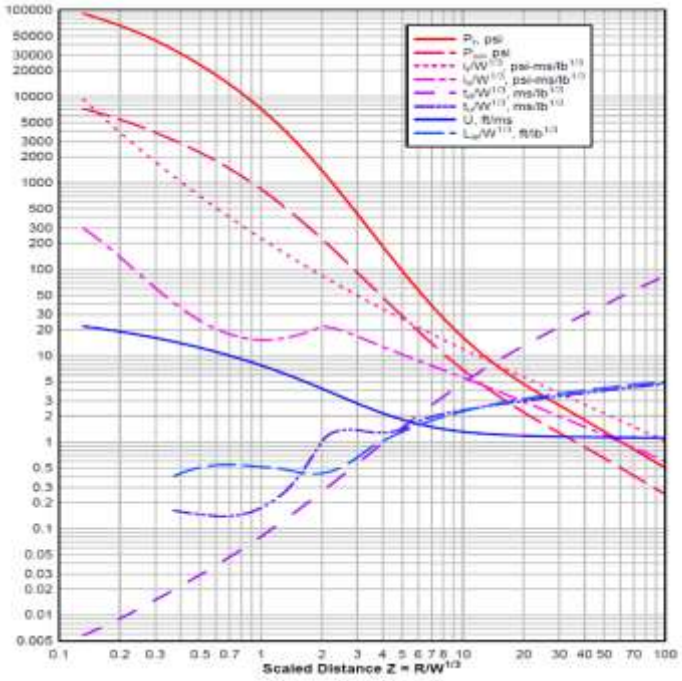

Fig. 1 Positive phase shock wave parameters for a spherical TNT explosion in free air at sea level [1]
Рис. 1 Параметри фази додатного тиску для вільного сферичного вибуху у повітрі тротилу на рівні моря [1]

M. Sadovskiy formulas [6, 7, 8] introduce similar relative distance parameter $\bar{R}$ (2):

$$\Delta P_f = \frac{0{,}084}{\bar{R}} + \frac{0{,}27}{\bar{R}^{\,2}} + \frac{0{,}7}{\bar{R}^{\,3}} \qquad (2)$$

For detonation point at 0.5m from the slab surface and 50kg TNT charge:

$$\bar{R}\ = \frac{R}{\sqrt[3]{C}} = \frac{0.5}{\sqrt[3]{50}} = 0.136$$

$$\Delta P_{\text{ф}} = \frac{0{,}084}{0.136} + \frac{0{,}27}{0.136^2} + \frac{0{,}7}{0.136^3} =$$

$$= 293.49MPa = 293490\ kPa$$

Similar values were calculated for detonation points at 1.0, 1.5, and 2.0 m from the slab surface. Results are presented in Fig. 9 and in the summary Table 1.

COMPUTATIONAL MODEL TO STUDY A FAILURE MECHANISM

Recent studies demonstrate that the evaluation of blast effects requires advanced numerical approaches capable of accurately reproducing shock wave propagation, nonlinear material response, and structural damage processes [14] . Using computational models to analyse damaged structures allows a transition from limit-stress assessment to the evaluating actual residual load-bearing capacity of elements after local failures [17].

Computational model was developed using ANSYS software package [14, 18, 19]. Material properties were defined using Engineering Data module, ANSYS DesignModeler was used to create geometry and numerical analysis was performed by Explicit Dynamics module based on ANSYS Mechanical.

To study failure mechanisms and summarize possible improvements first model was done as fully detailed hybrid 12x6m precast-steel floor with 12m cellular beams at 3m spacing and composite action provided. Slab thickness - 150 mm, concrete class - C35/40.

Beam considered to be produced by splitting and welding back together UKB 406×178×74 rolled I-section according to the British cross-section tables. Steel grade - S355, welded section depth - 576 mm, web openings diameter - 400 mm.

Slab considered precast with connecting reinforcement loops going around the headed shear studs welded to the steel cellular beam. Reinforcement loops are 16 mm in diameter and with B500B steel grade. Headed studs are 19 mm in diameter, 125mm heigh and are made with S235J2+C450 steel grade. Slab reinforcement loops spacing is same as welded studs spacing, which is equal to 305 mm.

Structural system was initially designed for a live load of 5 kN/m² and superimposed permanent load of 1 kN/m², which together with slab self-weight gives a total of 4.8 kN/m². Design was carried out according to EN 1994-1-1 (Eurocode 4) [20, 21, 22].

Model parameters:

- detonation point distance to the slab surface: 0.5 m;
- type of explosives: trinitrotoluene (TNT);
- amount of explosives: 50 kg shaped as cube with a side dimension of 313 mm (density 1630 kg/m³);
- computational limitation of the blast zone: 1.5 × 5.9 × 11.9 m measured from the lower flange of the beam;
- material behavior: elasto–plastic;
- failure criteria: relative strain of 0.15 for steel beams and welded studs, and 0.05 for reinforcement loops and reinforced concrete;
- additional element erosion criteria: element time step below $5x10^{-7}$c ($\Delta t = 0.9 \cdot (L/c)$, where L - diagonal or linear dimension of the element, and c – speed of sound in the material);
- total simulation time– 0,05c;
- maximum allowable element velocity: 14000 m/s (approximately twice the detonation velocity).

Model failure mechanism is shown in Fig. 2. Two specific deformation zones can be identified. Zone A of maximum overpressure, which pierces the slab leading to it's local destruction. And Zone B where due to different intensity of the overpressure slab separates from the steel beam and reinforcement loops disengage from the welded studs. Such division into areas with localized destruction and secondary damage is typical for blast and impact loading conditions [5, 23]. Studies of damage caused to protective structures by impact projectiles also suggest similar division into areas depending on type of failure [24].

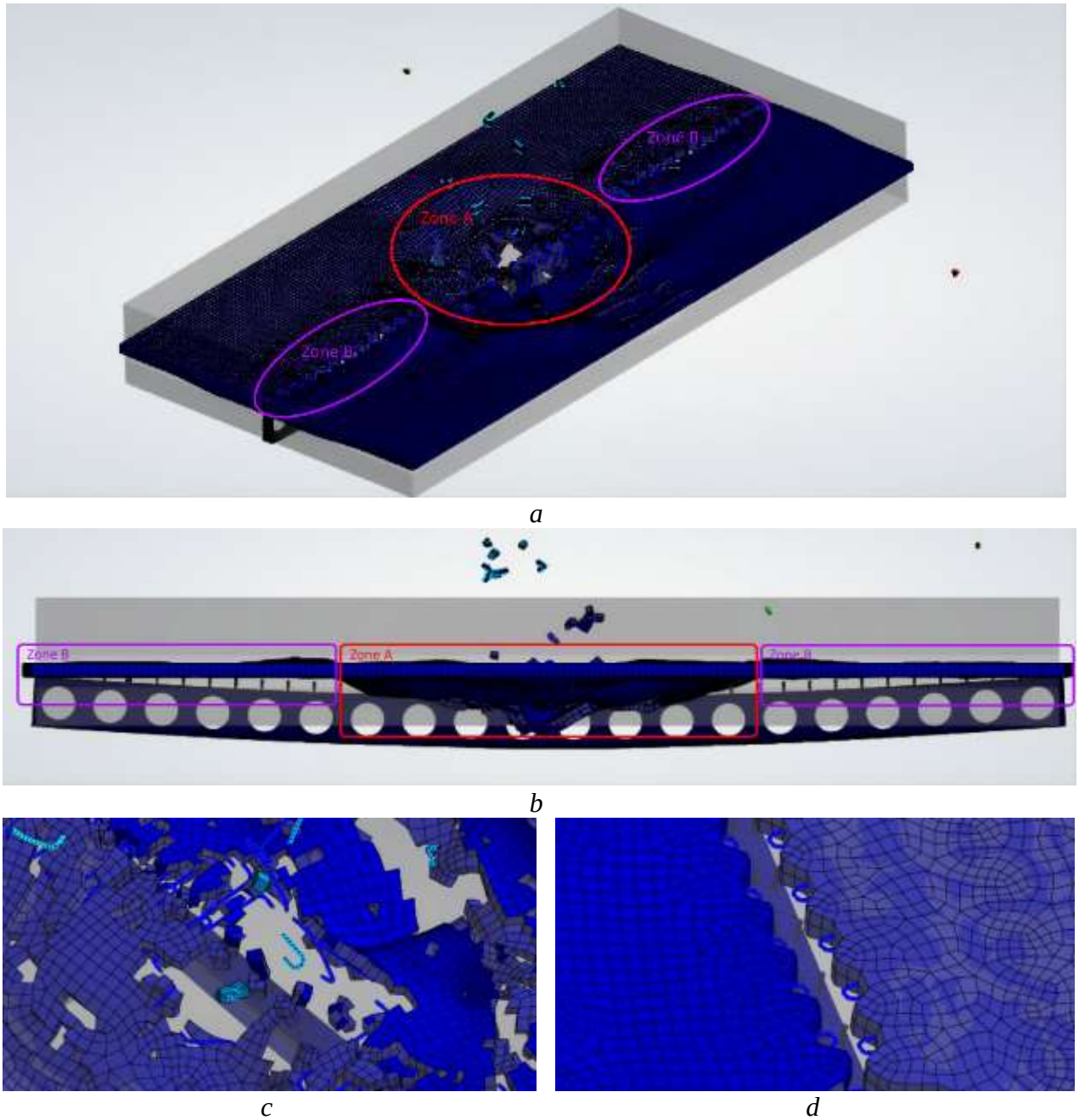

a

b

c *d*

Fig. 2 Failure mechanism with two typical zones A and B: *a* – outline of two typical zones, general view; *b* – outline of two typical zones, side view; c – Zone A type of failure detail; d – Zone B type of failure detail.

Рис. 2 Характер руйнування з двома характерними зонами А і Б: *a* – виокремлення двох характерних зон, загальний вид; *b* – виокремлення двох характерних зон, вид з боку*; c* – детальний вид руйнування у Зоні А*; d* – детальний вид руйнування у зоні Б.

Local penetration similar to Zone A can be seen as a result of Shahed-136 drone striking a boat with a metal hull (Fig. 3) [25]. In this case, more ductile, rib-stiffened deck limited the extent of damage. Therefore, two main directions for improving the structure in Zone A can be identified: increasing the deck thickness to prevent penetration, and/or adopting multi-element, highly robust structural systems to limit the damaged area. If penetration cannot be avoided, the structure must possess sufficient robustness limiting the damage (i.e., prevent progressive collapse).

Fig. 3 Penetration in metal boat hull as a result of being hit with a Shahed-136 drone [25] Photo by A. Bilyk

Рис. 3 Пробиття металевого корпусу човна як наслідок влучання дрону типу Shahed-136 [25] Автор фото А. Білик.

In cases where the structural system can be modified, this implies to use such solutions as continuous intersecting beam systems. When changes to the structural layout are not possible solution is to reduce beam span and spacing to limit the damaged floor area when 1–2 elements are excluded. This is consistent with the design concepts for protective structures based on damage localization and controlled redistribution of blast energy [26, 27]. Same logic is applied in modular reinforced-concrete protective structures, where each block functions as an autonomous element, limiting damage extents [28].

This research examines a specific structural system that intended to be improved but not fundamentally altered. Therefore, further research for Zone A will be focused on defining slab thicknesses sufficient to avoid floor system penetration at standard reinforcement ratios. Increasing thickness and introducing multi-layered elements is one of commonly used practices allowing to reduce blast-induced damage [19].

For Zone B problem is addressed by providing additional reinforcement or other local strengthening around the welded studs for pull-out resistance. The reinforcement may consist of straight or bent bars welded to the studs. These bars can be cast into the slab, enhance the local load-bearing capacity, and serve as a mechanical “lock” that restrains the reinforcement loops on the studs. Alternatively, various steel plates may be used to fix the studs and reinforcement loops together.

Model additionally indicated four important findings:

- charge shape affects how the blast wave is spreading and associated pressure distribution (Fig. 4);
- for detonation point at 0.5 m peak overpressure is reached within 0.01s (Fig. 5), so for up to four times larger distances (up to 2 m) a design time of 0.05s is used;

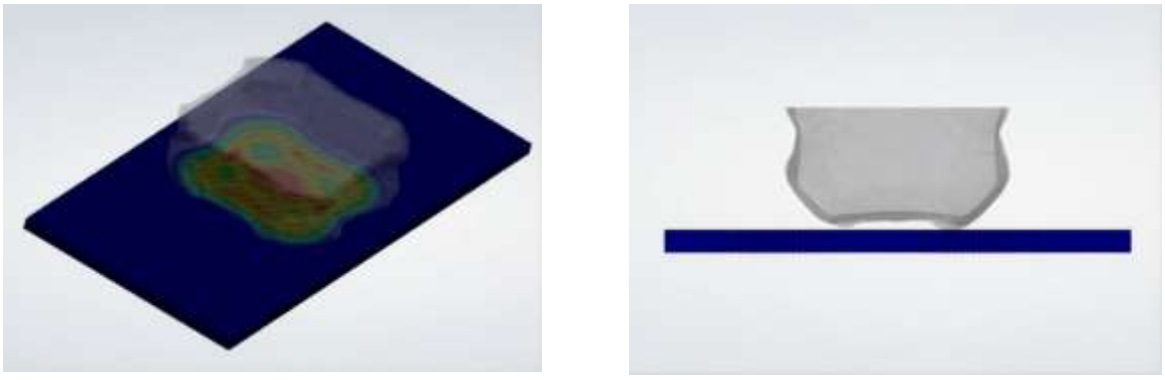

a *b*

Fig. 4 Charge shape effecting on how the shock wave is spreading: *a* – shock wave shape after detonation, general view*; b* - shock wave shape after detonation, side view.

Рис. 4 Вплив форми заряду на розповсюдження вибухової хвилі: *a* – розповсюдження вибухової хвилі після детонації, загальний вид*; b* – розповсюдження вибухової хвилі після детонації, вид з боку.

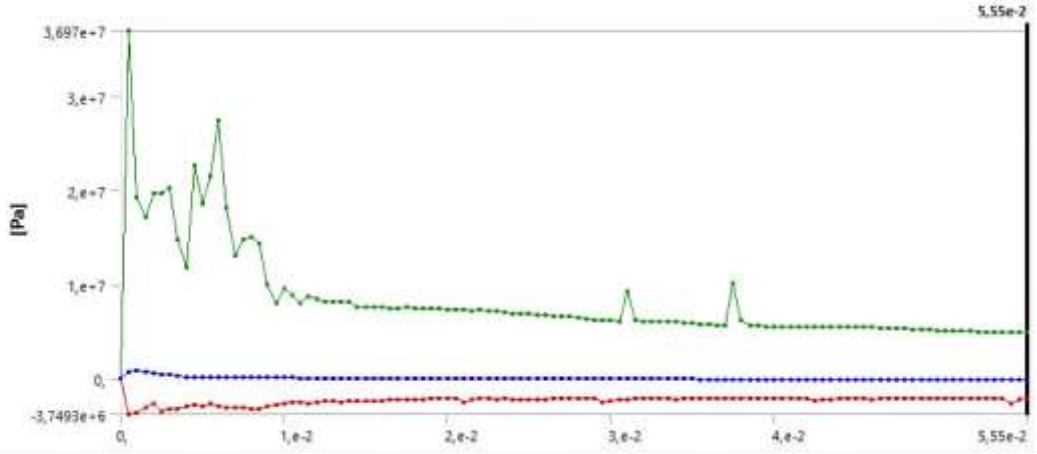

Fig. 5 Maximum pressure diagram over time of calculation
Рис. 5 Діаграма максимального тиску протягом часу розрахунку

- once the slab is locally damaged, the blast wave spreads into the space beneath the structure (Fig. 6);
- the pressure-time development curves closely match those found in other studies (Fig. 7).

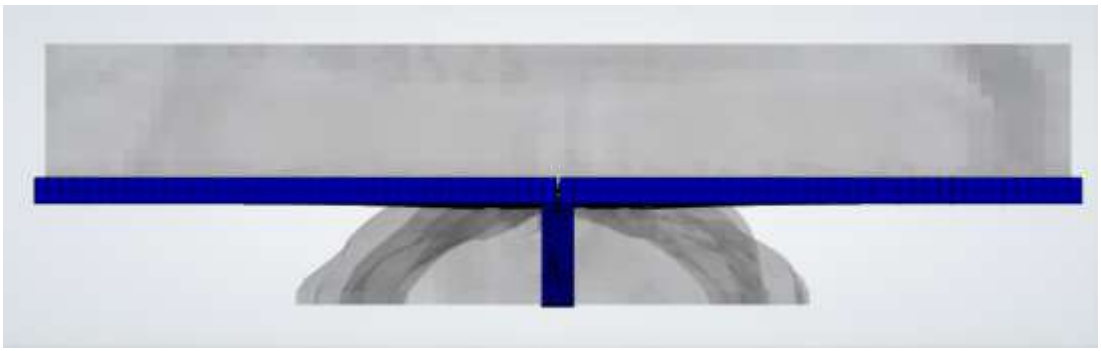

Fig. 6 Shock wave spreading into the space under the structure due to destruction/penetration of the floor slab
Рис. 6 Розповсюдження вибухової хвилі у простір під конструкцію через руйнування/пробиття плити перекриття

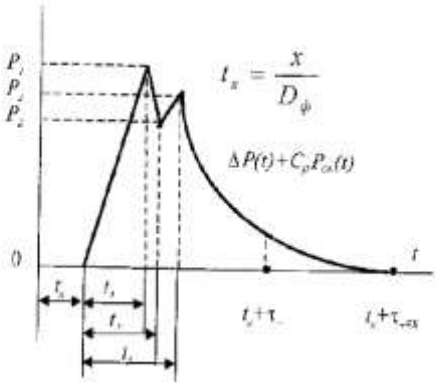

Рис. 7 Приклад зміни надлишкового тиску у часі, що наводяться в літературі
Fig. 7 Example of how pressure changes over time in literature sources

Developed model shown itself to be excessively complex for goal of assessing pressure on the structure. For simplification, beam web openings, headed studs, and reinforcement loops were excluded from further models. Composite action between beams and the slab was ensured by a *«bonded» (joined)* contact between beam top flanges and the underside of the slab. Further simplification all the way to plain slab is possible, but excluding structural deformations would affect pressure levels through deformation energy and geometrical non-linearity. From the energy standpoint, lower stiffness leads to lower

pressure and larger deformations, whereas higher stiffness results in higher pressure and smaller deformations. Geometric nonlinearity acts through surface curvature. So after first simulations it is decided to simplify model keeping general beam system and overall structural layout, considering two slab thicknesses (150 and 300mm) instead of one.

MODEL SERIES FOR PRESSURE ASSESMENT

In addition to simplifying models themselves, material failure criteria (strain or/and ultimate stress limits) were excluded, which made it possible to evaluate pressure acting onto undamaged structure. Only erosion criteria kept is a element time step limitation (excluding elements with time step below 5×10^{-7}s). This allowed to remove small and severely distorted elements that would otherwise reduce calculation speed substantially.

First stage included comparing results according to UFC 3-340-02 [1] and M. Sadovskiy formulas [6, 7, 8] with finite element simulations performed in Ansys [14, 18, 19] for a 50 kg TNT charge detonating at 0.5, 1.0, 1.5 and 2.0m from the surface of 150 and 300mm slabs. Pressure profiles example across and along a 6 × 12 m slab for a detonation point at 1.5 m are shown in Fig. 8.

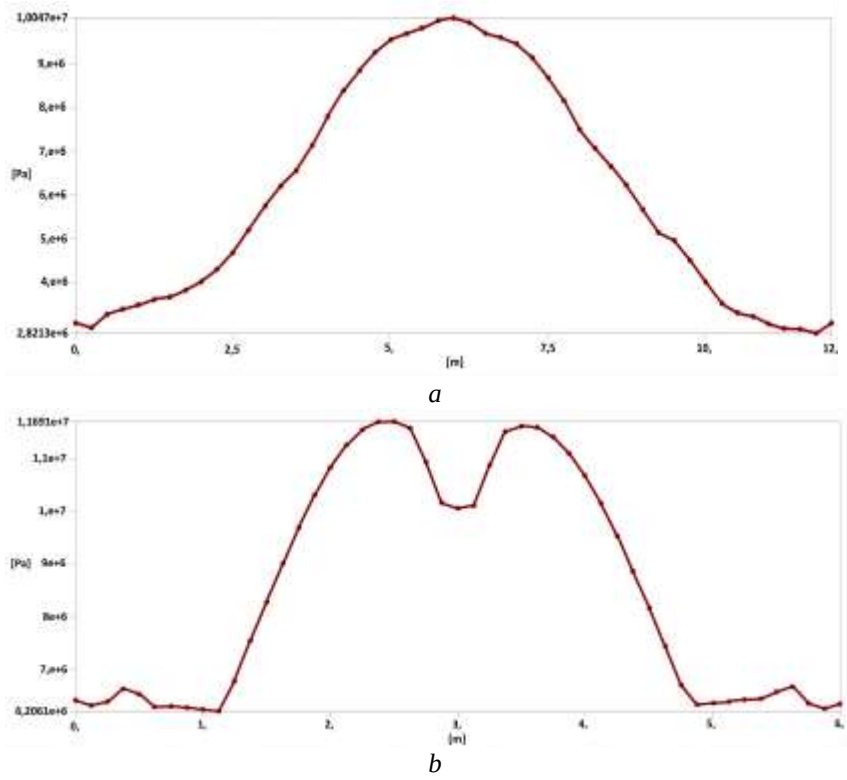

Fig. 8 Sample pressure profiles transverse and along the 6x12m slab: *a* – pressupre profile along the slab; *b* – pressure profile trasnverse to the slab.

Рис. 8 Приклади епюр розповсюдження тиску поперек та вздовж плити 6х12 м: *a*-епюра тиску вздовж плити; *b* – епюра тиску поперек плити.

After comparing pressure diagrams/profiles for 150 і 300mm slabs two key things were noted:

1. The peak pressure difference between the two slabs is significant (6.5–27.0%), with consistently higher values for the 300 mm slab. This indicates that the more flexible 150 mm slab dissipates more energy through deformation at lower pressure levels.
2. The stiffer 300 mm slab leads to increased pressure levels and reduced deformation-induced distortion of the pressure profiles/diagrams making stiffer 300mm preferable option for the further study. Structure's influence on blast-wave parameters confirms that slab is not a passive

element but actively modifies the nature of the explosive loading [29]. Since previous model series demonstrated an increase in pressure with increasing structural stiffness, it was proposed to further investigate the pressure response of a 300 mm slab on an ideally rigid base.

Results indicated similar pressure levels at shorter distances of 0.5 m and 1.0 m, but significantly lower values (by 43.5–55.4%) at distances of 1.5 m and 2.0 m. Pressure maps and distribution diagrams analysis revealed idealised rapid reflection of the blast wave slab on a rigid base, and a longer pressure growth and development phase for slabs supported by beams. This behaviour suggests deformation-induced "sail effect" generated by beam-supported slab systems. Similar deformation effects on pressure development have been reported for open-air blast scenarios [13, 30].

Five comparative data series were obtained as a result (Fig. 9). They confirm initial assumption that UFC 3-340-02 significantly overestimates peak overpressure by 4.49–7.00 times for the 150 mm slab on beams, by 3.54–6.58 times for the 300 mm slab on beams, and by 4.18–9.67 times for the 300 mm slab on a rigid base. M. Sadovskiy formulas [6, 7] show better agreement at detonation point distances of 1.5 and 2.0 m, with ratios ranging from 0.68 to 1.85 for different slab options. However, they still significantly overestimate pressure at shorter distances of 0.5 and 1.0 m, with factors ranging from 2.38 to 5.50.

Second stage included overpressure comparison for composite floor with only 300mm slab and detonation point distances of 0.5, 1.0, 1.5 and 2.0m with explosive charges of 50, 75 and 100 kg. Results were presented in Figs. 10-11 and summarised in Table 1. The key findings are:

1. The large discrepancies observed in the comparison with UFC 3-340-02 [1] and M. Sadovskiy formulas [6, 7, 8] are no longer evident. Obviously as a result of applying unified analysis/modelling approach.

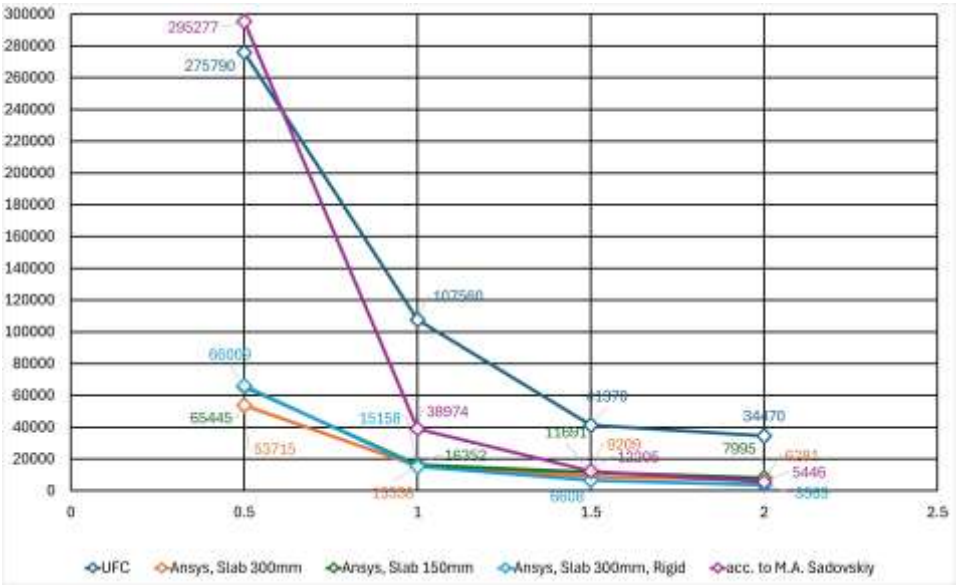

Fig. 9. Relationships between overpressure and the detonation point distance to the slab surface for a 50 kg charge

Рис. 9. Залежності надлишкового тиску від відстані епіцентру вибуху до перекриття для заряду у 50 кг.

2. At a fixed charge weight, detonation point distance influences peak overpressure in a nonlinear manner. Although the graph segments between 2 m and 1 m are close to linear and even nearly directly proportional, for

example, halving the distance (from 2 m to 1 m) increases the overpressure by 1.91–2.34 times. Thus, the exponential nature of the growth is primarily governed by the values obtained at the minimum stand-off distance of 0.5 m.

3. Dependence on amount of explosives is relatively close to proportional. For instance, doubling the charge mass (from 50 kg to 100 kg) results in an overpressure increase of 1.72–2.67 times.

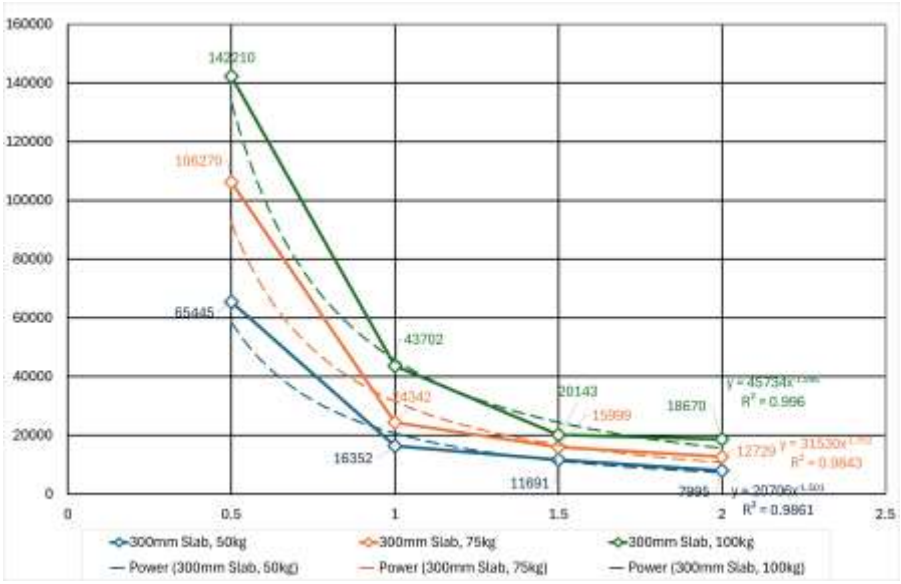

Fig. 10 Relationships (3.1-3.3) between overpressure and the detonation point distance to the slab surface for charges of 50, 75, and 100 kg.

Рис. 10 Залежності (3.1-3.3) надлишкового тиску від відстані епіцентру вибуху до перекриття для зарядів у 50, 75 і 100 кг

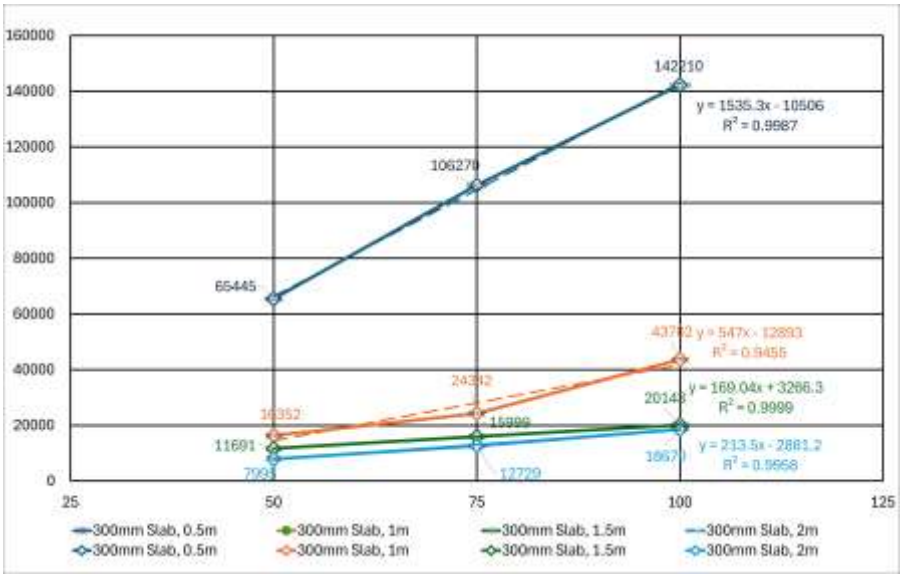

Fig. 11 Relationships (4.1-4.4) between overpressure and amount of explosives for a constant detonation point distance to the slab surface.

Рис. 11 Залежності (4.1-4.4) надлишкового тиску від кількості вибухової речовини при сталій відстані до перекриття

Table 1. Summary table of calculated overpressure acting on the slab
Таблиця 1. Зведена таблиця результатів розрахунків надлишкового тиску на плиту

Amount of explosives (TNT), kg	Detonation point distance to slab surface, m	Peak overpressure acting onto slab, Pa				
		UFC [1]	M. Sadovskiy formulas [6, 7, 8]	Ansys, 150mm slab + 600mm beams	Ansys, 300mm slab + 600mm beams	Ansys, 300mm slab + rigid base
50	0,5	275790	295277	42406	65445	66009
	1,0	107560	38974	14421	16352	15158
	1,5	41370	12205	8700	11691	6608
	2,0	34470	5446	5775	7995	3565
75	0,5	-	-	-	106270	-
	1,0	-	-	-	24342	-
	1,5	-	-	-	15999	-
	2,0	-	-	-	12729	-
100	0,5	-	-	-	142210	-
	1,0	-	-	-	43702	-
	1,5	-	-	-	20143	-
	2,0	-	-	-	18670	-

Graphs obtained for constant amount of explosives are well approximated by the following power functions (3-5):

$$\text{for 50kg: } P = 20.706 \cdot R^{-1.501} \quad (3)$$

$$\text{for 75kg: } P = 31.530 \cdot R^{-1.552} \quad (4)$$

$$\text{for 100kg: } P = 45.734 \cdot R^{-1.546} \quad (5)$$

where R – detonation point distance from the surface of the slab, in m;
P – peak overpressure, in kPa.

For constant detonation point distances and variable amount of explosives, linear relationships are sufficient (6-9):

$$\text{for 0.5m: } P = 1.535 \cdot W - 10.506 \quad (6)$$

$$\text{for 1.0m: } P = 0.547 \cdot W - 12.893 \quad (7)$$

$$\text{for 1.5m: } P = 0.169 \cdot W + 3.266 \quad (8)$$

$$\text{for 2.0m: } P = 0.214 \cdot W - 2.882 \quad (9)$$

where W – amount of explosives, in kg;
P – peak overpressure, in kPa.

Since the exponent in the distance-dependent expressions is consistently close to 1.5 (-1.546, -1.552, -1.503), while the mass dependence is approximately linear (exponent is 1). Therefore, instead of the scaled distance parameter $Z = R/\sqrt[3]{W}$ (1) adopted in UFC 3-340-02, a modified parameter $Z' = R^{1.5}/W$ (10) is suggested. The resulting dataset is shown graphically in Fig. 12. Approximation provides following expression for peak overpressure as a function of the modified scaled distance Z', in kPa (11):

$$P = 0.3719 \cdot Z'^{-1.034} \quad (11)$$

Alternatively, factors of distance-dependent equations will be expressed as functions of amount of explosives (Figs. 13 and 14). Distance-based relationships are selected to be referential due to their consistent functional similarity.

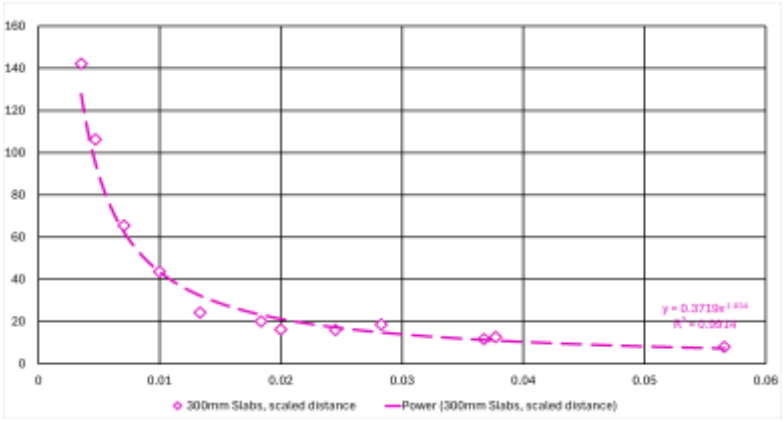

Fig. 12 Relationship (6) between overpressure and the modified scaled distance parameter Z' (10).
Рис.12 Залежності (6) надлишкового тиску від параметру модифікованої відносної відстані $Z'(10)$

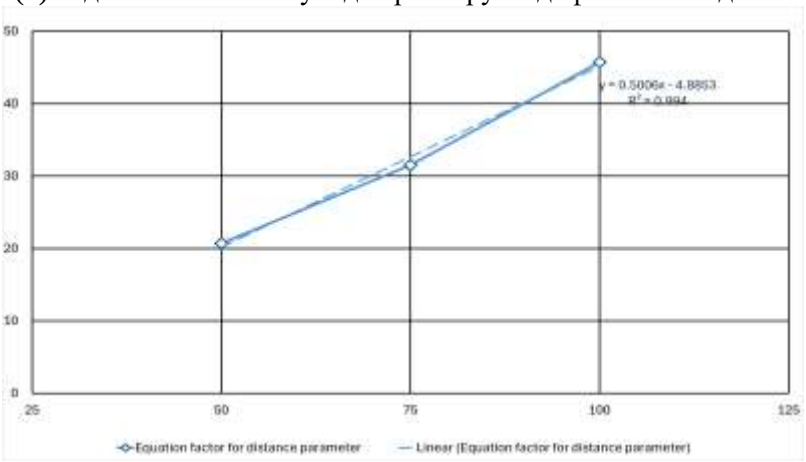

Fig. 13 Approximation of relationship between factor and the amount of explosives
Рис. 13 Апроксимація залежності коефіцієнту від кількості вибухової речовини

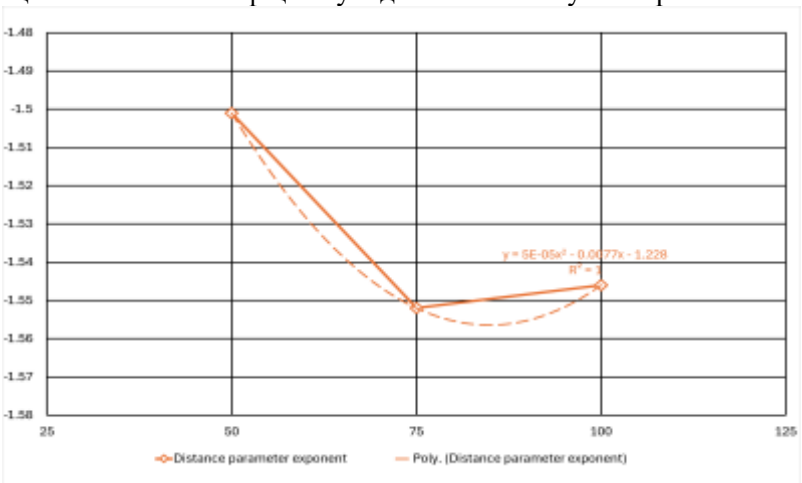

Fig. 14 Approximation of relationship between the function exponent and the amount of explosives
Рис. 14 Апроксимація залежності ступеню функції від кількості вибухової речовини

As a result, the following alternative expression is obtained (12):

$$P = (0.5006 \cdot W - 4.8853) \times \times R^{0.00005 \cdot W^2 - 0.0077 \cdot W - 1.228} \quad (12)$$

A simplified analytical form is additionally suggested (13):

$$P = (0.50 \cdot W - 4.89) \cdot R^{-1.50} \quad (13)$$

Obtained relationships (3-5, 6-9, 10, 11, 12) are verified in summary Tables 2 and 3.

Table 2. Verification of the obtained relationships.
Таблиця 2. Перевірка отриманих залежностей

Amount of explosives (TNT), kg	Detonation point distance to slab surface, m	Peak overpressure acting onto slab, Pa						
		Ansys	Distance function (3-5)	Deviation	Amount of explosives function (6-9)	Deviation	Modified scaled distance function (11)	Deviation
50	0.5	65445	58606.0	-10.4%	66259.0	1.2%	62238.4	-4.9%
	1	16352	20706.0	26.6%	14457.0	-11.6%	21240.3	29.9%
	1.5	11691	11266.3	-3.6%	11718.3	0.2%	11325.1	-3.1%
	2	7995	7315.6	-8.5%	7793.8	-2.5%	7248.8	-9.3%
75	0.5	106270	92453.3	-13.0%	104641.5	-1.5%	94653.6	-10.9%
	1	24342	31530.0	29.5%	28132.0	15.6%	32302.8	32.7%
	1.5	15999	16804.7	5.0%	15944.3	-0.3%	17223.5	7.7%
	2	12729	10752.9	-15.5%	13131.3	3.2%	11024.1	-13.4%
100	0.5	142210	133546.2	-6.1%	143024.0	0.6%	127445.3	-10.4%
	1	43702	45734.0	4.6%	41807.0	-4.3%	43493.7	-0.5%
	1.5	20143	24434.4	21.3%	20170.3	0.1%	23190.4	15.1%
	2	18670	15662.0	-16.1%	18468.8	-1.1%	14843.2	-20.5%

Table 3. Verification of the obtained alternative relationships.
Таблиця 3. Перевірка отриманих альтернативних залежностей

Amount of explosives (TNT), kg	Detonation point distance to slab surface, m	Peak overpressure acting onto slab, Pa						
		Ansys	Distance function + approximation (7)	Deviation	Distance function + approximation, simplified (8)	Deviation	Final (9)	Deviation
50	0.5	65445	56505.9	-13.7%	56879.7	-13.1%	65410.2	-0.1%
	1	16352	20144.7	23.2%	20110.0	23.0%	23126.0	41.4%
	1.5	11691	11018.9	-5.7%	10946.5	-6.4%	12588.2	7.7%
	2	7971	7181.7	-9.9%	7110.0	-10.8%	8529.8	7.0%
75	0.5	106270	93941.4	-11.6%	92235.0	-13.2%	106068.8	-0.2%
	1	24342	32659.7	34.2%	32610.0	34.0%	37501.0	54.1%
	1.5	15999	17603.7	10.0%	17750.6	10.9%	20413.0	27.6%
	2	12729	11354.5	-10.8%	11529.4	-9.4%	13612.2	6.9%
100	0.5	142210	127596.3	-10.3%	127590.3	-10.3%	146727.5	3.2%
	1	43702	45174.7	3.4%	45110.0	3.2%	51876.0	18.7%
	1.5	20143	24609.9	22.2%	24554.8	21.9%	28237.7	40.2%
	2	18670	15993.8	-14.3%	15948.8	-14.6%	18694.5	0.1%

The simplified distance-dependent approximation (13) provides the best balance between minimising negative errors and ease of practical application. To prevent unconservative predictions, a safety coefficient of 1.15 is introduced (14), corresponding to a maximum negative deviation of 14.6%:

$$P = 1.15 \cdot (0.50 \cdot W - 4.89) \cdot R^{-1.50} = (0.575 \cdot W - 5.624) \cdot R^{-1.50} \quad (14)$$

CONCLUSIONS

When studying separate blast loading affects and parameters it is recommended to simplify models within technically justified limits due to high computational resource requirements for blast analysis.

Future research should utilize spherical charges to ensure more idealised and physically consistent blast-wave spread.

Results confirm that UFC 3-340-02 [1] and M. Sadovskiy formulas [6, 7, 8] overestimate peak overpressure at small detonation point distances. This does not indicate deficiencies in the methodologies themselves but rather limits their applicability to structural assessment at larger distances.

Key practical result is the proposed relationship for peak overpressure on steel beam-supported slabs at distances up to 2 m, consistent with the stated research purpose.

An important finding was the identification of a linear, yet not strictly proportional, relationship between peak overpressure and amount of explosives, as well as a nonlinear dependence on detonation point distance.

Furthermore, important observations were made in relation to failure mechanisms of prefabricated steel–concrete hybrid/composite floor systems under blast loading. This allowed to define first strategies for improving structural blast resistance. These include increasing slab thickness and implementing measures to prevent pull-out failure of headed studs from the slab.

Next prioritized research task is to define how thick a slabs with standard reinforcement levels should be to prevent blast-induced local penetration. This will involve calculating slabs of different thickness within reasonable practical limits for blast loading at a minimum detonation point distance of 0.5m. For each amount of explosives (50, 75 and 100kg) a certain minimum slab thickness will be determined as a result.

Reinforcement bars locally welded to the shear studs appear to be the most rational solution for preventing stud pull-out failure. Reinforcing bar may be placed and welded during installation in the case of a single-row stud arrangement. For double-row stud layout, the reinforcing bar may be either casted into the slab along the seam or otherwise be made as short links between adjacent studs/loops.

ETHICAL DECLARATIONS

The authors have no relevant financial or non-financial interests to report.

LITERATURE

1. **Department of Defense** (2008). UFC 3-340-02: Structures to resist the effects of accidental explosions. *Washington, DC: U.S. Department of Defense, 1867 p.*
2. **European Committee fo**r Standardization (2025). EN 1991-1-7:2025 Eurocode 1 – Actions on structures – Part 1-7: Accidental actions. *Brussels: CEN, 80 p, [Current, since 20.07.2025].*
3. Міністерство регіонального розвитку, будівництва та житлово-комунального господарства України (2019). ДБН В.1.2-4:2019 Інженерно-технічні заходи цивільного захисту. *Київ: Мінрегіон України, 28 с, [Чинний з 01.08.2019].*
4. **Shuaib, M. & Daoud, O.** (2015). Numerical Modelling of Reinforced Concrete Slabs under Blast Loads of Close-in Detonations Using the Lagrangian Approach. *Journal of Physics: Conference Series. 628.* https://doi.org/10.1088/1742-6596/628/1/012065
5. **Abebe, S., & Mohammed, T. A.** (2022). Performance assessment of reinforced concrete frame under close-in blast loading. *Advances in Civil Engineering, 2022,* 3979195. https://doi.org/10.1155/2022/3979195
6. **Барабаш, М., Костира, Н., Максименко, В., & Бармін, І.** (2023). Моделювання динамічних навантажень вибухового типу в задачах дослідження міцності будівельних конструкцій з використанням ПК ЛІРА-САПР. *Наука та будівництво, 4(38), 20-27.* https://doi.org/10.33644/2313-6679-4-2023-3
7. **Каплюк, О., Нікітченко, В., Кірдей, Л., Терновський, А., & Брайко, В.** (2022). Особливості дослідження боєпри-пасів з термобаричними вибуховими речови-нами.4 *Збірник наукових праць Державного науково-дослідного інституту випробувань і сертифікації озброєння та військової техніки, 1(11), 55–65.* https://doi.org/10.37701/dndivsovt.11.2022.07

8. **Mykhailovskyi, D., Skliarov, I., & Komar, O.** (2025). Comparison of methods for calculating the parameters of an explosion shock wave for the design of protective engineering structures. *Building Constructions. Theory and Practice*, (16), 110–123. https://doi.org/10.32347/2522-4182.16.2025.110-123
9. **Ромашкіна, М., Пісаревський, Б., & Журавльов, О. (2024)**. Розрахунок будівлі на вплив дії повітряної ударної хвилі прямим динамічним методом з використанням ПК ЛІРА-САПР. *Будівельні конструкції. Теорія і практика, (14), 147–160.* https://doi.org/10.32347/2522-4182.14.2024.147-160
10. **Dusenberry, D. (Ed.). (2010).** Handbook for blast resistant design of buildings. *John Wiley & Sons*, 484 p. https://doi.org/10.1002/9780470549070
11. **Liu, J., Gao, C., Sun, Z., & Yin, J. (2024).** On the estimation of near-field air blast peak overpressure from cylindrical charges. *International Journal of Protective Structures, 15*(3), 442–454. https://doi.org/10.1177/20414196231177358
12. ***Ma, R., Wang, X., You, S., Sun, Z., & Huang, F. (2025).*** Experimental and numerical analysis of near-field detonation products and shock wave characteristics for cylindrical charge. *Journal of Dynamic Behavior of Materials*, 53, 242-258. https://doi.org/10.1016/j.jdbm.2025.100212
13. **Rigby, S. E., Knighton, R., Clarke, S. D., & Tyas, A.** (2020). Reflected near-field blast pressure measurements using high-speed video. *Experimental Mechanics, 60, 875–888.* https://doi.org/10.1007/s11340-020-00615-3
14. **Gudadappanavar, B., Selvakumar, M., Yeole M. M., Hosur, V. A., Dibdalli, Y., Morales-Verdejo, C. & Sunagar, P.** (2026). Explicit-dynamics assessment of reinforced concrete frame response under TNT blast: Stand-off, charge weight and incidence angle effects. *SSRG International Journal of Civil Engineering*, 13(3), 255–273. https://doi.org/10.14445/23488352/IJCE-V13I3P119
15. **Михайловський, Д., Білик, А., & Скляров, І.** (2024). Розрахунок конструкцій будівель і споруд на дії основних факторів ураження засобів повітряного нападу: *монографія. Київ: Каравела, 92 с.* ISBN 978-960-801-874-7
16. **Білик, А., Коваль, М., Коваль, В., & Коцюруба, В.** (2023). Організаційно-технічні засади побудови системи інженерного захисту об'єктів критичної інфраструктури енергетичної галузі України. *Наука і оборона, (3–4), 11-16 с.* https://doi.org/10.33099/2618-1614-2022-20-3-4-11-16
17. **Барабаш, М., Костира, Н., & Томашевський, А.** (2022). Визначення напружено-деформованого стану та міцності пошкоджених несучих конструкцій інструментами ПК «ЛІРА-САПР». *Український журнал будівництва та архітектури, 1(007), 7–14 с.* https://doi.org/10.30838/J.BPSACEA.2312.220222.7.827
18. **Nyström, U.** (2013). Modelling of concrete structures subjected to blast and fragment loading. *Göteborg: Chalmers University of Technology, Department of Civil and Environmental Engineering, 107 p.* ISBN 978-91-7385-805-2
19. **Zuievska, N., Darmostuk, D., Semchuk, R., & Zuievskyi, Y.** (2025). Modelling blast effects for a multilayer "Reinforced-concrete slab–Soil mass" system. *Geo-Technical Mechanics*, 175, 152–168. https://doi.org/10.15407/geotm2025.175.152
20. **European Committee** for Standardization. (2004). EN 1994-1-1:2004 Eurocode 4 – Design of composite steel and concrete structures – Part 1-1: General rules and rules for buildings. *Brussels: CEN, 118 p., [Current, since 27.05.2004].*
21. **Dujmović, D., Androić, B., & Lukačević, I.** (2015). Composite structures according to Eurocode 4: Worked examples. *Berlin: Wilhelm Ernst & Sohn, 924 p.* https://doi.org/10.1002/9783433604908
22. **Дмитренко, Є.** (2021). Моделювання сумісної роботи сталевих балкових конструкцій із залізобетонними ребристими плитами перекриття. *Будівельні конструкції. Теорія і практика, 1(8), 44–57.* https://doi.org/10.32347/2522-4182.8.2021.44-57
23. **Kumar, V., Kartik, K. V., & Iqbal, M. A.** (2020). Experimental and numerical investigation of reinforced concrete slabs under blast loading. *Engineering Structures, 206, 110125.* https://doi.org/10.1016/j.engstruct.2019.110125
24. **Білик, С., & Білик, А.** (2024). Порівняння методик проникнення дії засобів повітряного

нападу противника в залізобетонні конструкції споруд захисту об'єктів критичної інфраструктури. *Сучасні будівельні конструкції з металу та деревини: Збірник наукових праць, 28, 75–83 с.* https://doi.org/10.31650/2707-3068-2024-28

25. **Коваль, М., Коваль, В., Білик, А., Коцюруба, В., & Кубраков, О.** (2023). Основи інженерного захисту об'єктів критичної інфраструктури енергетичної галузі України від засобів повітряного нападу противника (за ред. А. С. Білика). *Київ: Генеральний штаб Збройних Сил України, 185 с.* ISBN 978-617-520-660-7
26. **Ngo, T., Mendis, P., Gupta, A., & Ramsay, J.** (2007). Blast loading and blast effects on structures – An overview. Electronic *Journal of Structural Engineering, Special Issue: Loading on Structures, 76–91.* https://doi.org/10.56748/ejse.671
27. **Гетун, Г., Колякова, В., Безклубенко, І., & Соломін, А.** (2023). Конструктивні рішення вибухостійких будівель з приміщеннями цивільного захисту населення. *Будівельні конструкції. Теорія і практика, (13), 41–50.* https://doi.org/10.32347/2522-4182.13.2023.41-50
28. **Roth, M. J., & Slawson, T. R.** (2004). Design and validation of modular, reinforced concrete bunkers. *Vicksburg, MS: U.S. Army Corps of Engineers, Engineer Research and Development Center, 8 p.* https://apps.dtic.mil/sti/tr/pdf/ADA433005.pdf
29. **Lin, S.-C., Gao, S., & Han, J.-Q.** (2011). Effect of the reinforced concrete slab on the blast shock wave properties, *Combustion, Explosion, and Shock Waves, 56, 731-740 с.* https://doi.org/10.1134/S0010508220060131
30. ***Chi, M., Jiang, H., Lan, X., Xu, T., & Jiang, Y.*** (2021). Study on overpressure propagation law of vapor cloud explosion. *ACS Omega, 6(49), 34003–34020 p.* https://doi.org/10.1021/acsomega.1c05332

REFERENCES

1. **Department of Defense** (2008). UFC 3-340-02: Structures to resist the effects of accidental explosions. *Washington, DC: U.S. Department of Defense, 1867 p.*
2. **European Committee** for Standardization (2025). EN 1991-1-7:2025 Eurocode 1 – Actions on structures – Part 1-7: Accidental actions. *Brussels: CEN, 80 p, [Current, since 20.07.2025].*
3. Ministerstvo rehionalnoho rozvytku, budivnytstva ta zhytlovo-komunalnoho hospodarstva Ukrainy (2019). DBN V.1.2-4:2019 Inzhenerno-tekhnichni zakhody tsyvilnoho zakhystu. *Kyiv: Minrehion Ukrainy, 28 s., [Chynnyi z 01.08.2019].* [in Ukrainian]
4. **Shuaib, M. & Daoud, O.** (2015). Numerical Modelling of Reinforced Concrete Slabs under Blast Loads of Close-in Detonations Using the Lagrangian Approach. *Journal of Physics: Conference Series. 628.* https://doi.org/10.1088/1742-6596/628/1/012065
5. **Abebe, S., & Mohammed, T. A.** (2022). Performance assessment of reinforced concrete frame under close-in blast loading. *Advances in Civil Engineering, 2022,* 3979195. https://doi.org/10.1155/2022/3979195
6. **Barabash, M. S., Kostyra, N. O., Maksymenko, V. P., & Barmin, I. V.** (2023). Modeliuvannia dynamichnykh navantazhen vybukhovoho typu v zadachakh doslidzhennia mitsnosti budivelnykh konstruktsii z vykorystanniam PK LIRA-SAPR. *Nauka ta budivnytstvo, 4(38), 20-27.* [in Ukrainian] https://doi.org/10.33644/2313-6679-4-2023-3
7. **Kapliuk, O. M., Nikitchenko, V. I., Kirdei, L. M., Ternovskyi, A. Yu., & Braiko, V. V.** (2022). Osoblyvosti doslidzhennia boieprypasiv z termobarychnymy vybukhovymy rechovynamy. *Zbirnyk naukovykh prats Derzhavnoho naukovo-doslidnoho instytutu vyprobuvan i sertyfikatsii ozbroiennia ta viiskovoi tekhniky, 1(11), 55–65.* [in Ukrainian] https://doi.org/10.37701/dndivsovt.11.2022.07
8. **Mykhailovskyi, D., Skliarov, I., & Komar, O.** (2025). Comparison of methods for calculating the parameters of an explosion shock wave for the design of protective engineering structures. *Building Constructions. Theory and Practice, (16), 110–123.* [in Ukrainian] https://doi.org/10.32347/2522-4182.16.2025.110-123
9. **Romashkina, M., Pisarevskyi, B., & Zhuravlov, O.** (2024). Rozrakhunok budivli na vplyv dii povitrianoi udarnoi khvyli priamym dynamichnym metodom z vykorystanniam PK LIRA-SAPR. *Budivelni konstruktsii. Teoriia i praktyka, (14), 147–160.* [in Ukrainian] https://doi.org/10.32347/2522-4182.14.2024.147-160
10. **Dusenberry, D. (Ed.). (2010).** Handbook for blast resistant design of buildings. *John Wiley & Sons,* 484 p. https://doi.org/10.1002/9780470549070

11. **Liu, J., Gao, C., Sun, Z., & Yin, J. (2024).** On the estimation of near-field air blast peak overpressure from cylindrical charges. *International Journal of Protective Structures, 15*(3), 442–454. https://doi.org/10.1177/20414196231177358
12. ***Ma, R., Wang, X., You, S., Sun, Z., & Huang, F. (2025).*** Experimental and numerical analysis of near-field detonation products and shock wave characteristics for cylindrical charge. *Journal of Dynamic Behavior of Materials*, 53, 242-258. https://doi.org/10.1016/j.jdbm.2025.100212
13. **Rigby, S., Knighton, R., Clarke, S., & Tyas, A.** (2020). Reflected near-field blast pressure measurements using high-speed video. *Experimental Mechanics, 60, 875–888.* https://doi.org/10.1007/s11340-020-00615-3
14. **Gudadappanavar, B., Selvakumar, M., Yeole M., Hosur, V., Dibdalli, Y., Morales-Verdejo, C. & Sunagar, P.** (2026). Explicit-dynamics assessment of reinforced concrete frame response under TNT blast: Stand-off, charge weight and incidence angle effects. *SSRG International Journal of Civil Engineering, 13(3),* 255–273. https://doi.org/10.14445/23488352/IJCE-V13I3P119
15. **Mykhailovskyi, D., Bilyk, A., & Skliarov, I.** (2024). Rozrakhunok konstruktsii budivel i sporud na dii osnovnykh faktoriv urazhennia zasobiv povitrianoho napadu: *monohrafiia. Kyiv: Karavela, 92 s.* [in Ukrainian] ISBN 978-960-801-874-7
16. **Bilyk, A., Koval, M., Koval, V., & Kotsiuruba, V.** (2023). Orhanizatsiino-tekhnichni zasady pobudovy systemy inzhenernoho zakhystu obiektiv krytychnoi infrastruktury enerhetychnoi haluzi Ukrainy. *Nauka i oborona, (3–4), 11–16.* [in Ukrainian] https://doi.org/10.33099/2618-1614-2022-20-3-4-11-16
17. **Barabash, M., Kostyra, N., & Tomashevskyi, A.** (2022). Vyznachennia napruzheno-deformovanoho stanu ta mitsnosti poshkodzhenykh nesuchykh konstruktsii instrumentamy PK LIRA-SAPR. *Ukrainskyi zhurnal budivnytstva ta arkhitektury, 1(007), 7–14.* [in Ukrainian] https://doi.org/10.30838/J.BPSACEA.2312.220222.7.827
18. **Nyström, U.** (2013). Modelling of concrete structures subjected to blast and fragment loading. *Göteborg: Chalmers University of Technology, Department of Civil and Environmental Engineering, 107 p.* ISBN 978-91-7385-805-2
19. **Zuievska, N., Darmostuk, D., Semchuk, R., & Zuievskyi, Y.** (2025). Modelling blast effects for a multilayer "Reinforced-concrete slab–Soil mass" system. *Geo-Technical Mechanics,* 175, 152–168. https://doi.org/10.15407/geotm2025.175.152
20. European Committee for Standardization. (2004). EN 1994-1-1:2004 Eurocode 4 – Design of composite steel and concrete structures – Part 1-1: General rules and rules for buildings. *Brussels: CEN, 118 p., [Current, since 27.05.2004].*
21. **Dujmović, D., Androić, B., & Lukačević, I.** (2015). Composite structures according to Eurocode 4: Worked examples. *Berlin: Wilhelm Ernst & Sohn, 924 p.* https://doi.org/10.1002/9783433604908
22. **Dmytrenko, Ye.** (2021). Modeliuvannia sumisnoi roboty stalevykh balkovykh konstruktsii iz zalizobetonnymy rebrystymy plytamy perekryttia. *Budivelni konstruktsii. Teoriia i praktyka, 1(8), 44–57.* [in Ukrainian] https://doi.org/10.32347/2522-4182.8.2021.44-57
23. **Kumar, V., Kartik, K. V., & Iqbal, M. A.** (2020). Experimental and numerical investi-gation of reinforced concrete slabs under blast loading. *Engineering Structures, 206, 110125.* https://doi.org/10.1016/j.engstruct.2019.110125
24. **Bilyk, S., & Bilyk, A.** (2024). Porivniannia metodyk pronyknennia dii zasobiv povitrianoho napadu protyvnyka v zalizobetonni konstruktsii sporud zakhystu obiektiv krytychnoi infrastruktury. *Suchasni budivelni konstruktsii z metalu ta derevyny: Zbirnyk naukovykh prats, 28, 75–83.* [in Ukrainian] https://doi.org/10.31650/2707-3068-2024-28
25. **Koval, M., Koval, V., Bilyk, A., Kotsiuruba, V., & Kubrakov, O.** (2023). Osnovy inzhenernoho zakhystu obiektiv krytychnoi infrastruktury enerhetychnoi haluzi Ukrainy vid zasobiv povitrianoho napadu protyvnyka (za red. A. S. Bilyka). *Kyiv: Heneralnyi shtab Zbroinykh Syl Ukrainy, 185 s.* [in Ukrainian] ISBN 978-617-520-660-7
26. **Ngo, T., Mendis, P., Gupta, A., & Ramsay, J.** (2007). Blast loading and blast effects on structures – An overview. Electronic *Journal of Structural Engineering, Special Issue: Loading on Structures, 76–91.* https://doi.org/10.56748/ejse.671
27. **Getun, H., Koliakova, V., Bezklubenko, I., & Solomin, A.** (2023). Konstruktyvni rishennia

vybukhostiikykh budivel z prymishchenniamy tsyvilnoho zakhystu naselennia. *Budivelni konstruktsii. Teoriia i praktyka, (13), 41–50.* [in Ukrainian]https://doi.org/10.32347/2522-4182.13.2023.41-50

28. **Roth, M., & Slawson, T.** (2004). Design and validation of modular, reinforced concrete bunkers. *Vicksburg, MS: U.S. Army Corps of Engineers, Engineer Research and Development Center, 8 p.* https://apps.dtic.mil/sti/tr/pdf/ADA433005.pdf
29. **Lin, S., Gao, S., & Han, J.** (2011). Effect of the reinforced concrete slab on the blast shock wave properties, *Combustion, Explosion, and Shock Waves, 56, 731-740 c.* https://doi.org/10.1134/S0010508220060131
30. ***Chi, M., Jiang, H., Lan, X., Xu, T., & Jiang, Y.*** (2021). Study on overpressure propagation law of vapor cloud explosion. *ACS Omega, 6(49), 34003–34020 p* https://doi.org/10.1021/acsomega.1c05332

ПОРІВНЯННЯ НАДЛИШКОВОГО ТИСКУ НА ПЕРЕКРИТТЯ ПРИ ВИБУХУ НА МАЛИХ ВІДСТАНЯХ ВІД ЙОГО ПОВЕРХНІ

Микита БІЛЯЄВ

Анотація. Стаття присвячена дослідженню надлишкового тиску, що діє на перекриття будівель у разі вибуху, який відбувається на малих відстанях від його поверхні. Актуальність роботи зумовлена тим, що чинні нормативні методики та розрахункові залежності, зокрема положення стандарту UFC 3-340-02 та формул М. А. Садовського, орієнтовані переважно на більші відстані від епіцентру вибуху й не враховують локальний характер навантаження, що виникає у випадку близького підриву. Це потенційно призводить до значних похибок при оцінюванні реального рівня вибухового впливу на елементи конструкцій.

Метою дослідження є побудова та апроксимація реалістичної залежності пікового надлишкового тиску від відстані до поверхні перекриття та маси вибухової речовини для вибухів на висоті до 2 м. Для досягнення цієї мети виконано серію числових експериментів із використанням програмного комплексу Ansys. Розрахункова модель представляє збірне сталезалізобетонне перекриття розміром 12×6 м по металевих балках з перфорованою стінкою, спочатку з урахуванням усіх конструктивних елементів, а в подальшому - у спрощеному вигляді з різною товщиною плити. Розглянуто вибухи тротилового еквіваленту масою 50, 75 та 100 кг на відстанях 0,5; 1,0; 1,5 і 2,0 м від поверхні.

Отримані результати показали, що нормативні методики суттєво завищують значення пікового тиску при малих відстанях: за UFC 3-340-02 - у 4–9 разів, за формулами М. А. Садовського - у 2–5 разів порівняно з числовим моделюванням. Виявлено істотний вплив жорсткості перекриття на величину тиску. Встановлено, що залежність тиску від відстані має виражений нелінійний характер, тоді як залежність від маси вибухової речовини є майже лінійною.

На основі отриманих даних запропоновано нові аналітичні залежності для оцінювання пікового надлишкового тиску, зокрема узагальнену формулу через параметр відносної відстані, адаптовану до малих дистанцій. Запропоновані вирази пройшли перевірку за серіями числових експериментів і можуть використовуватися для інженерної оцінки вибухового навантаження на перекриття при близьких підривах. Додатково проаналізовано характер руйнування конструкції та визначено основні напрями її підсилення: збільшення товщини плити та удосконалення анкерування сталевих балок з метою запобігання відриву.

Ключові слова: вибуховий вплив; сталезалізобетонні конструкції; комбіновані конструкції; перфоровані балки; надлишковий тиск.

Received: *March 23, 2026.*
Revised: *April 20, 2026.*
Accepted: *May 28, 2026*